Networks and Heterogeneous Media

https://www.aimspress.com/journal/nhm

NHM, 21(5): 1950–1967.
DOI: 10.3934/nhm.2026073
Received: 06 June 2026
Revised: 14 September 2026
Accepted: 17 September 2026
Published: 28 September 2026

Research article

A high-order unconditionally stable scheme for time-fractional telegraph equations with generalized alternating numerical fluxes: Analysis and properties

Miaomiao Yang* **and Xiao Chen**

School of General Education, Zhengzhou Business University, Zhengzhou 451200, China

* **Correspondence:** Email: mathxinxi@163.com.

Abstract: This paper introduces and examines a flexible numerical strategy for solving the time-fractional telegraph equation. A finite difference scheme is used for temporal discretization, while spatial discretization is achieved using a discontinuous Galerkin method that incorporates generalized alternating numerical fluxes. From an implementation standpoint, these generalized alternating fluxes offer enhanced flexibility and greater adaptability compared with conventional flux selections. We prove that the resulting numerical scheme is unconditionally stable and convergent. Several numerical examples are provided to demonstrate the robustness, reliability, and accuracy of the proposed method.

Keywords: fractional calculus; numerical scheme; generalized alternating numerical fluxes; stability

1. Introduction

Fractional partial differential equations (FPDEs) extend classical integer-order partial differential equations by incorporating derivatives of noninteger order. Owing to this unique characteristic, FPDEs have been widely applied in numerous fields, such as engineering, physics, and various areas of the applied sciences. These equations are especially useful for modeling complex physical phenomena that involve memory effects and hereditary properties—features that conventional integer-order models frequently cannot fully capture.

More concretely, FPDEs are well-suited for describing nonlocal relationships that arise in systems governed by power-law memory kernels in both time and space. Consequently, they enable the modeling of materials or processes where past states significantly influence future behavior. This type of behavior is particularly important for describing media with memory, such as viscoelastic materials and certain biological systems [1].

The incorporation of fractional derivatives also allows FPDEs to capture long-range interactions, which are essential in many physical systems, including anomalous diffusion, wave propagation, and

heat conduction in heterogeneous media. Beyond these traditional contexts, fractional calculus has proven valuable in fluid dynamics, materials science, and biological systems, offering a more refined and accurate framework for characterizing phenomena involving fractal geometry, complex rheological responses, and nonstandard diffusion behavior [2].

To efficiently handle the resulting fractional models, numerous numerical strategies have been developed over the years. For example, finite difference schemes have attracted considerable attention and have been thoroughly analyzed in works such as [3–7]. Likewise, discontinuous Galerkin (DG) methods [8–11], finite element approaches [12], spectral techniques [13–15], and collocation-based methods [16, 17] have all emerged as powerful and flexible tools for the numerical investigation of FPDEs. These methodological advances underscore the growing importance of computational techniques in addressing the inherent complexities of fractional-order systems. It is now widely acknowledged that noninteger order integrals and derivatives provide a robust mathematical framework for capturing essential material properties, including nonlocality, long-term memory behavior, and fractal characteristics.

The telegraph equations constitute a class of hyperbolic partial differential equations with applications in various scientific domains, such as signal analysis, wave propagation, random walk theory, and related fields. Considerable research has been devoted to the study of time-fractional telegraph equations [18]. In particular, Beghin and Orsingher [19] investigated the fractional telegraph equation and showed that its fundamental solution can be interpreted as the density associated with a particular composition of stochastic processes. Subsequently, Orsingher and Beghin [20] further examined the fundamental solutions of this equation. Chen et al. [21] derived analytical solutions for the fractional telegraph equation using the method of separation of variables. Meanwhile, Momani [22] applied Adomian decomposition methods to obtain both analytic and approximate solutions for the same class of equations. Jiang and Lin [23] derived series-form exact solutions via the reproducing kernel theorem. Biazar et al. [24] explored the variational iteration method as a means to solve the fractional telegraph equation. Additionally, Yildirim [25] applied the Adomian decomposition method and the homotopy perturbation method to address fractional telegraph equations. In recent years, increasing attention has also been devoted to high-order numerical methods for time-fractional telegraph and diffusion–wave equations. Zhang and Wang [26] developed compact finite difference schemes for time-fractional diffusion–wave equations with time delay, obtaining $(3-\alpha)$-th order accuracy in time and fourth-order accuracy in space for $1 < \alpha < 2$. Their analysis also established the stability and convergence of the proposed schemes. More recently, Ou et al. [27] proposed a second-order fitted scheme for two-dimensional nonlinear time-fractional telegraph equations with initial singularity. By combining the $L2\text{-}1_\sigma$ approximation with a time two-grid technique, their method achieves second-order accuracy in both time and space while improving computational efficiency for nonlinear problems. These studies demonstrate the continuing interest in developing stable and high-order temporal discretizations for fractional telegraph-type equations.

The DG method combines many of the advantageous features of both finite element and finite volume approaches, making it a highly attractive technique for solving partial differential equations. Its appeal largely arises from the great flexibility it offers in mesh design and the choice of shape functions, as well as its capacity to achieve high-order accuracy in the numerical solution [28]. In the

present work, we consider the following time-fractional telegraph equation of order α with $1 < \alpha < 2$:

$$\begin{aligned} &\frac{\partial^\alpha T(x,t)}{\partial t^\alpha} + \frac{\partial^{\alpha-1} T(x,t)}{\partial t^{\alpha-1}} + \rho_1 T(x,t) = \rho_2 T_{xx} + f(x,t), \qquad (x,t) \in (a,b) \times (0, t_F], \\ &T(x,0) = T_0(x), \quad \frac{\partial T(x,0)}{\partial t} = T_1(x), \qquad x \in [a,b], \end{aligned} \tag{1.1}$$

where $\frac{\partial^\alpha T(x,t)}{\partial t^\alpha}$ and $\frac{\partial^{\alpha-1} T(x,t)}{\partial t^{\alpha-1}}$ denote the Caputo fractional derivatives with respect to the time variable t. The constants ρ_1 and ρ_2 are positive parameters, while x and t represent the spatial and temporal coordinates, respectively. Periodic boundary conditions are assumed throughout this paper. For a given order δ with $K - 1 < \delta < K$ ($K \in \mathbb{N}$), the Caputo fractional derivative $\frac{\partial^\delta T(x,t)}{\partial t^\delta}$ is defined as follows [29]:

$$\frac{\partial^\delta T(x,t)}{\partial t^\delta} = \frac{1}{\Gamma(K-\delta)} \int_0^t \frac{\partial^K T(x,s)}{\partial s^K} \frac{ds}{(t-s)^{1-K+\delta}},$$

where $\Gamma(\cdot)$ denotes the standard Gamma function.

The remainder of this paper is organized as follows: Section 2 presents an overview of the essential notation and relevant theoretical preliminaries. In Section 3, we develop a combined finite difference and DG method for the time-fractional telegraph equation, accompanied by a thorough discussion of the stability properties and a detailed error analysis. Section 4 presents a series of numerical experiments designed to illustrate the convergence accuracy and practical effectiveness of the proposed scheme. Finally, the last section offers some concluding remarks.

2. Notation and theoretical preliminaries

Let $\Omega = \bigcup_{j=1}^N I_j$ be a decomposition of the interval $\Omega = [a,b]$, where each subinterval is given by $I_j = [x_{j-\frac{1}{2}}, x_{j+\frac{1}{2}}]$ for $j = 1, 2, \ldots, N$. For each cell, the length is defined as $\Delta x_j = x_{j+\frac{1}{2}} - x_{j-\frac{1}{2}}$ with $1 \le j \le N$, and we denote the maximum mesh size as $h = \max_{1 \le j \le N} \Delta x_j$.

The set of all cell interfaces (the mesh skeleton) is denoted by

$$\Gamma_h = \bigcup_{j=1}^N \partial I_j = \left\{ x_{\frac{1}{2}}, x_{\frac{3}{2}}, \ldots, x_{N+\frac{1}{2}} \right\}.$$

For a piecewise smooth function v, we define the interface norm by

$$\|v\|^2_{L^2(\Gamma_h)} = \sum_{j=1}^N \left(\left| v^-_{j+\frac{1}{2}} \right|^2 + \left| v^+_{j+\frac{1}{2}} \right|^2 \right),$$

where the traces at the endpoints are understood periodically.

At the interface point $x_{j+\frac{1}{2}}$, we introduce $u^+_{j+\frac{1}{2}}$ and $u^-_{j+\frac{1}{2}}$ to represent the traces taken from the right neighboring cell I_{j+1} and the left cell I_j, respectively. The DG finite element space of degree up to k is then denoted by V_h^k, consisting of piecewise polynomials defined separately on each cell

$$V_h^k = \left\{ v : v\big|_{I_j} \in P^k(I_j), \quad j = 1, 2, \ldots, N \right\}.$$

We now introduce the generalized Gauss–Radau projection, which will play a fundamental role in the convergence analysis presented later.

For a periodic function ψ defined on the interval $[a, b]$, its generalized Gauss–Radau projection, denoted $\mathcal{P}_\theta\psi$, is uniquely determined following the construction in [30]. The corresponding projection error is defined as $\psi^e = \mathcal{P}_\theta\psi - \psi$. For any parameter $\theta \neq \frac{1}{2}$, this projection satisfies the following properties on each mesh cell I_j with $j = 1, 2, \ldots, N$:

$$\int_{I_j} \psi^e v\, dx = 0, \quad \forall v \in P^{k-1}(I_j), \qquad \text{and} \qquad (\psi^e)^{(\theta)}_{j+\frac{1}{2}} = 0. \tag{2.1}$$

Based on these defining conditions, the following approximation estimate can be established (see [31, 32]).

Lemma 2.1. *Assume $\theta \neq \frac{1}{2}$ and let $\psi \in H^{s+1}[a, b]$. Then the projection error ψ^e satisfies the bound*

$$\|\psi^e\| + h^{\frac{1}{2}}\|\psi^e\|_{L^2(\Gamma_h)} \leq Ch^{\min(k+1,s+1)}\|\psi\|_{s+1}, \tag{2.2}$$

where the positive constant C is independent of both the mesh size h and the function ψ.

Throughout this paper, the symbol C denotes a generic constant whose value may change from one occurrence to another. We adopt the standard notation commonly used in Sobolev space theory. The inner product on $L^2(E)$ is written as $(\cdot, \cdot)_E$, with the corresponding norm denoted by $\|\cdot\|_E$. When $E = \Omega$, the subscript E is omitted for brevity.

3. The scheme

Throughout this section, we assume that the fractional order satisfies $1 < \alpha < 2$, and hence $0 < \alpha - 1 < 1$. Accordingly, the Caputo derivatives of orders α and $\alpha - 1$ correspond to $K = 2$ and $K = 1$, respectively, in the general definition given above.

In this section, we first introduce a finite difference scheme for approximating the time-fractional derivatives. We then construct a fully implicit discrete system, where the spatial derivatives are treated using the DG method. Detailed stability and convergence analyses of the proposed scheme are provided.

Consider a partition of the time interval $[0, t_F]$ as follows:

$$0 = t_0 < t_1 < \cdots < t_{n-1} < t_n = t_F,$$

with a uniform time step size $\Delta t = t_F/M$, where $M \in \mathbb{N}$. The discrete time levels are defined by $t_n = n\Delta t$ for $n = 0, 1, \ldots, M$. The discretization procedure first targets the time-fractional derivative of order α, and subsequently addresses the derivative of order $\alpha - 1$.

Let

$$v(x, t) = \frac{\partial T(x, t)}{\partial t}.$$

According to the prescribed initial conditions in Eq (1.1), we have

$$T(x, t_0) = T_0(x), \qquad v(x, t_0) = T_1(x).$$

For $i \geq 1$, we use the second-order backward difference formula

$$v(x,t_i) = \frac{3T(x,t_i) - 4T(x,t_{i-1}) + T(x,t_{i-2})}{2\Delta t} + \gamma_1^i, \tag{3.1}$$

where, under the required temporal regularity of T, $|\gamma_1^i| \leq C(\Delta t)^2$.

It should be noted that when $i = 1$, Formula (3.1) involves the auxiliary value $T(x,t_{-1})$. To initialize the scheme consistently with the prescribed initial derivative $T_t(x,0) = T_1(x)$, we introduce the ghost value

$$T^{-1}(x) = T^0(x) - \Delta t\, T_1(x), \tag{3.2}$$

where $T^0(x) = T_0(x)$. Thus, T^{-1} is not an additional initial condition, but an auxiliary starting value determined completely by the given initial data.

Specifically, the time-fractional derivative of order α is expressed as

$$\begin{aligned}
\frac{\partial^\alpha T(x,t_n)}{\partial t^\alpha} &= \frac{1}{\Gamma(2-\alpha)} \int_0^{t_n} \frac{\partial v(x,\tau)}{\partial \tau} \frac{d\tau}{(t_n-\tau)^{\alpha-1}} \\
&= \frac{1}{\Gamma(2-\alpha)} \sum_{i=0}^{n-1} \int_{t_i}^{t_{i+1}} \frac{\partial v(x,\tau)}{\partial \tau} \frac{d\tau}{(t_n-\tau)^{\alpha-1}} \\
&= \frac{1}{\Gamma(2-\alpha)} \sum_{i=0}^{n-1} \int_{t_i}^{t_{i+1}} \frac{v(x,t_{i+1}) - v(x,t_i)}{\Delta t} \frac{d\tau}{(t_n-\tau)^{\alpha-1}} + \gamma_2^n \\
&= \frac{(\Delta t)^{1-\alpha}}{\Gamma(3-\alpha)} \Bigg[\frac{3T(x,t_n) - 4T(x,t_{n-1}) + T(x,t_{n-2})}{2\Delta t} \\
&\qquad + \sum_{i=1}^{n-1} (b_{n-i} - b_{n-i-1}) \frac{3T(x,t_i) - 4T(x,t_{i-1}) + T(x,t_{i-2})}{2\Delta t} \\
&\qquad - b_{n-1} v(x,t_0) \Bigg] + \gamma_3^n.
\end{aligned} \tag{3.3}$$

For the time-fractional derivative of order $\alpha - 1$, denoted $\frac{\partial^{\alpha-1} T(x,t_n)}{\partial t^{\alpha-1}}$, a similar derivation (see [15]) yields the following discrete approximation after straightforward algebraic manipulations:

$$\frac{\partial^{\alpha-1} T(x,t_n)}{\partial t^{\alpha-1}} = \frac{(\Delta t)^{1-\alpha}}{\Gamma(3-\alpha)} \sum_{i=0}^{n-1} b_i (T(x,t_{n-i}) - T(x,t_{n-i-1})) + \gamma_4^n, \tag{3.4}$$

where the coefficients are defined as

$$b_0 = 1, \qquad b_i = (i+1)^{2-\alpha} - i^{2-\alpha}, \quad i = 1,2,3,\ldots$$

Following the same reasoning as in [15], the resulting truncation errors satisfy the bounds

$$|\gamma_3^n| \leq C(\Delta t)^{3-\alpha}, \qquad |\gamma_4^n| \leq C(\Delta t)^{3-\alpha}.$$

Moreover, the coefficients $\{b_i\}$ possess the following useful properties:

$$\begin{aligned}
&b_i > 0, \quad i = 1,2,\ldots,n; \\
&1 = b_0 > b_1 > b_2 > \cdots > b_n, \quad \text{and} \quad b_n \to 0 \text{ as } n \to \infty.
\end{aligned} \tag{3.5}$$

For Eq (1.1), we begin by converting it into an equivalent first-order system. Specifically, we introduce an auxiliary variable to represent the spatial derivative, which yields the following formulation:

$$p = T_x, \qquad \frac{\partial^\alpha T(x,t)}{\partial t^\alpha} + \frac{\partial^{\alpha-1} T(x,t)}{\partial t^{\alpha-1}} + \rho_1 T(x,t) - \rho_2\, p_x = f(x,t). \tag{3.6}$$

Let $\beta = 2(\Delta t)^\alpha \Gamma(3-\alpha)$. We aim to find approximate solutions $T_h^n, p_h^n \in V_h^k$ such that for any test functions $\phi, w \in V_h^k$, the following discrete variational formulation holds:

$$\begin{aligned}
&\int_\Omega (\rho_1 + 3 + 2\Delta t) T_h^n \phi\, dx + \beta\rho_2 \left(\int_\Omega p_h^n \phi_x\, dx - \sum_{j=1}^{N} \left((\widehat{p_h^n}\phi^-)_{j+\frac{1}{2}} - (\widehat{p_h^n}\phi^+)_{j-\frac{1}{2}} \right) \right) \\
&\qquad = \sum_{i=1}^{n-1} (b_{n-i-1} - b_{n-i}) \int_\Omega (3T_h^i - 4T_h^{i-1} + T_h^{i-2})\phi\, dx \\
&\qquad\quad + 2\Delta t\, b_{n-1} \int_\Omega v_h^0 \phi\, dx + 4 \int_\Omega T_h^{n-1} \phi\, dx - \int_\Omega T_h^{n-2} \phi\, dx \\
&\qquad\quad + 2\Delta t \sum_{i=1}^{n-1} (b_{n-i-1} - b_{n-i}) \int_\Omega T_h^i \phi\, dx \\
&\qquad\quad + 2\Delta t\, b_{n-1} \int_\Omega T_h^0 \phi\, dx + \beta \int_\Omega f^n \phi\, dx, \\
&\int_\Omega p_h^n w\, dx + \int_\Omega T_h^n w_x\, dx - \sum_{j=1}^{N} \left((\widehat{T_h^n} w^-)_{j+\frac{1}{2}} - (\widehat{T_h^n} w^+)_{j-\frac{1}{2}} \right) = 0.
\end{aligned} \tag{3.7}$$

The quantities denoted by a hat ($\widehat{T_h^n}$ and $\widehat{p_h^n}$) appearing in the boundary integral terms originate from the integration–by–parts procedure and are referred to as *numerical fluxes*. The appropriate selection of these fluxes plays a crucial role not only in the stability analysis but also in the overall effectiveness of the DG formulation. In the present work, we use the generalized alternating numerical fluxes, which offer enhanced flexibility and broader applicability compared with conventional flux choices. These fluxes are specified as follows:

$$\widehat{T_h^n} = \theta (T_h^n)^- + (1-\theta)(T_h^n)^+, \qquad \widehat{p_h^n} = (1-\theta)(p_h^n)^- + \theta (p_h^n)^+, \tag{3.8}$$

where the parameter θ is taken from the set $\left[0, \frac{1}{2}\right) \cup \left(\frac{1}{2}, 1\right]$. The specific value $\theta = \frac{1}{2}$ is deliberately excluded, since it yields a symmetric flux that renders the analysis of uniqueness and approximation properties more challenging, particularly in connection with the underlying generalized Gauss–Radau projection.

Next, without sacrificing generality, we set $f = 0$ in the theoretical analysis for the sake of simplicity.

Theorem 3.1. *The fully discrete DG scheme (3.7) is unconditionally stable. Moreover, a positive constant C exists, depending only on T, t_F, and α, such that for all time levels $n = 1, 2, \ldots, M$, the following estimate holds:*

$$\|T_h^n\| \le C(\|T_h^0\| + \Delta t\, \|T_1(x)\|). \tag{3.9}$$

Proof. We now proceed with the stability analysis. In the discrete scheme (3.7), we select the test functions as $\phi = T_h^n$ and $w = \beta\rho_2 p_h^n$. Together with the numerical fluxes defined in Eq (3.8), we obtain the following identity:

$$\begin{aligned}(\rho_1 + 3 + 2\Delta t)\|T_h^n\|^2 + \beta\rho_2\|p_h^n\|^2 + \beta\rho_2 \sum_{j=1}^{N} \big(&F_1(T_h^n, p_h^n)_{j+\frac{1}{2}} \\ &- F_1(T_h^n, p_h^n)_{j-\frac{1}{2}} + F_2(T_h^n, p_h^n)_{j-\frac{1}{2}}\big) \\ = &\sum_{i=1}^{n-1}(b_{n-i-1} - b_{n-i}) \int_\Omega (3T_h^i - 4T_h^{i-1} + T_h^{i-2})T_h^n \, dx \\ &+ 2\Delta t\, b_{n-1} \int_\Omega v_h^0 T_h^n \, dx + 4\int_\Omega T_h^{n-1} T_h^n \, dx - \int_\Omega T_h^{n-2} T_h^n \, dx \\ &+ 2\Delta t \sum_{i=1}^{n-1}(b_{n-i-1} - b_{n-i}) \int_\Omega T_h^i T_h^n \, dx + 2\Delta t\, b_{n-1} \int_\Omega T_h^0 T_h^n \, dx,\end{aligned} \tag{3.10}$$

where the auxiliary terms are given by

$$\begin{aligned}F_1(T_h^n, p_h^n) =&(p_h^n)^-(T_h^n)^- - (p_h^n)^+(T_h^n)^- - (T_h^n)^-(p_h^n)^-, \\ F_2(T_h^n, p_h^n) =&\theta\big((p_h^n)^-(T_h^n)^- - (p_h^n)^+(T_h^n)^+ - (p_h^n)^+(T_h^n)^- + (p_h^n)^+(T_h^n)^+ \\ &- (T_h^n)^-(p_h^n)^- + (T_h^n)^-(p_h^n)^+\big) + (1-\theta)\big((p_h^n)^+(T_h^n)^+ - (p_h^n)^-(T_h^n)^- \\ &- (p_h^n)^-(T_h^n)^+ + (p_h^n)^-(T_h^n)^- - (T_h^n)^+(p_h^n)^+ + (T_h^n)^+(p_h^n)^-\big).\end{aligned}$$

After straightforward algebraic manipulation, we know $F_2(T_h^n, p_h^n) = 0$.

Moreover, after summing over all elements, the remaining interface terms in $F_1(T_h^n, p_h^n)$ form a telescoping sum. Owing to the periodic boundary condition and the complementary structure of the generalized alternating numerical fluxes, the corresponding interface contribution vanishes exactly.

From Eq (3.10), applying the Cauchy–Schwarz inequality, we derive the estimate

$$\begin{aligned}(\rho_1+3 + 2\Delta t)\|T_h^n\|^2 \le &\sum_{i=1}^{n-1}(b_{n-i-1} - b_{n-i})(3\|T_h^i\| + 4\|T_h^{i-1}\| + \|T_h^{i-2}\|)\|T_h^n\| \\ &+ 2\Delta t\, b_{n-1}\|v_h^0\|\|T_h^n\| + 4\|T_h^{n-1}\|\|T_h^n\| + \|T_h^{n-2}\|\|T_h^n\| \\ &+ 2\Delta t \sum_{i=1}^{n-1}(b_{n-i-1} - b_{n-i})\|T_h^i\|\|T_h^n\| + 2\Delta t\, b_{n-1}\|T_h^0\|\|T_h^n\|.\end{aligned}$$

Simplifying with the factor $\|T_h^n\|$, we arrive at

$$\begin{aligned}\|T_h^n\| \le &\sum_{i=1}^{n-1}(b_{n-i-1} - b_{n-i})(3\|T_h^i\| + 4\|T_h^{i-1}\| + \|T_h^{i-2}\|) \\ &+ 2\Delta t\, b_{n-1}\|v_h^0\| + \frac{4}{3}\|T_h^{n-1}\| + \|T_h^{n-2}\| \\ &+ \sum_{i=1}^{n-1}(b_{n-i-1} - b_{n-i})\|T_h^i\| + b_{n-1}\|T_h^0\|.\end{aligned} \tag{3.11}$$

We now establish the boundedness of $\|T_h^n\|$ via mathematical induction. The base case $n = 1$ follows from Eq (3.11) as

$$\|T_h^1\| \leq 2\Delta t\|v_h^0\| + \frac{7}{3}\|T_h^0\| + \|T_h^{-1}\|.$$

To estimate the auxiliary starting value T_h^{-1}, for any $\phi \in V_h^k$

$$\int_{I_j} T_h^{-1}\phi\, dx = \int_{I_j} T_h^0\phi\, dx - \Delta t \int_{I_j} T_1(x)\phi\, dx.$$

Choosing $\phi = T_h^{-1}$ and applying the Cauchy–Schwarz and Young inequalities, we obtain

$$\int_{I_j} T_h^{-1}\phi\, dx = \int_{I_j} \mathbb{P}(T(x,0) - \Delta t\, T_1(x))\phi\, dx = \int_{I_j} T_h^0\phi\, dx - \Delta t \int_{I_j} T_1(x)\phi\, dx, \quad \forall \phi \in V_h^k.$$

Choosing $\phi = T_h^{-1}$ and applying Young's inequality gives

$$\begin{aligned}\|T_h^{-1}\|_{I_j}^2 &= \int_{I_j} T_h^0 T_h^{-1} dx - \Delta t \int_{I_j} T_1(x) T_h^{-1} dx \\ &\leq \|T_h^0\|_{I_j}^2 + \frac{1}{4}\|T_h^{-1}\|_{I_j}^2 + (\Delta t)^2\|T_1(x)\|_{I_j}^2 + \frac{1}{4}\|T_h^{-1}\|_{I_j}^2.\end{aligned}$$

Summing over all cells $j = 1, \ldots, N$ yields

$$\|T_h^{-1}\| \leq C(\|T_h^0\| + \Delta t\|T_1(x)\|). \tag{3.12}$$

A similar argument leads to the bound for the initial velocity approximation

$$\|v_h^0\| \leq \|T_1(x)\|. \tag{3.13}$$

Substituting Eqs (3.12) and (3.13) into the estimate for $n = 1$, we obtain

$$\|T_h^1\| \leq C(\|T_h^0\| + \Delta t\|T_1(x)\|).$$

Now assume that for all indices $m = 1, 2, 3, \ldots, J$, the following uniform bound holds:

$$\|T_h^m\| \leq C(\|T_h^0\| + \Delta t\|T_1(x)\|). \tag{3.14}$$

Consider $n = J + 1$ in Eq (3.11). Then

$$\begin{aligned}\|T_h^{J+1}\| \leq &\sum_{i=1}^{J}(b_{J-i} - b_{J+1-i})(3\|T_h^i\| + 4\|T_h^{i-1}\| + \|T_h^{i-2}\|) \\ &+ 2\Delta t\, b_J\|v_h^0\| + \frac{4}{3}\|T_h^J\| + \|T_h^{J-1}\| \\ &+ \sum_{i=1}^{J}(b_{J-i} - b_{J+1-i})\|T_h^i\| + b_J\|T_h^0\|.\end{aligned}$$

Applying the induction hypothesis together with the identity

$$\sum_{i=1}^{J}(b_{i-1}-b_i)+b_J=1,$$

we immediately deduce

$$\|T_h^{J+1}\| \le C(\|T_h^0\| + \Delta t\|T_1(x)\|).$$

Thus, by induction, the claimed stability estimate holds for all n. This completes the proof of Theorem 3.1. □

Theorem 3.2. *Assume that the exact solution $T(x,t_n)$ of Problem (1.1) is sufficiently smooth with bounded partial derivatives up to a certain order, and let T_h^n be the numerical solution obtained from the fully discrete DG scheme (3.7). Then a positive constant C exists, independent of both the time step size Δt and the mesh size h, such that the following error estimate holds:*

$$\|T(x,t_n)-T_h^n\| \le C(h^{k+1}+(\Delta t)^{3-\alpha}).$$

Proof. Since periodic boundary conditions are imposed throughout this paper, the exact solution and the numerical solution are understood to satisfy the corresponding periodicity at the endpoints $x=a$ and $x=b$. Accordingly, in the following error analysis, $\mathcal{P}_\theta$ and $\mathcal{P}_{1-\theta}$ denote the generalized Gauss–Radau projections defined under the periodic boundary condition.

We begin by introducing the following decomposition of the errors:

$$\begin{aligned} e_T^n &= T(x,t_n)-T_h^n=\xi_T^n-\eta_T^n, \qquad \xi_T^n=\mathcal{P}_\theta e_T^n, \qquad \eta_T^n=\mathcal{P}_\theta T(x,t_n)-T(x,t_n),\\ e_p^n &= p(x,t_n)-p_h^n=\xi_p^n-\eta_p^n, \qquad \xi_p^n=\mathcal{P}_{1-\theta} e_p^n, \qquad \eta_p^n=\mathcal{P}_{1-\theta}p(x,t_n)-p(x,t_n). \end{aligned} \tag{3.15}$$

Here, $\mathcal{P}_\theta$ denotes the generalized Gauss–Radau projection operator, which plays a crucial role in the subsequent convergence analysis.

By choosing the numerical fluxes as defined in Eq (3.8), we obtain the following error equation:

$$\begin{aligned} &(\rho_1+3+2\Delta t)\int_\Omega e_T^n\phi\,dx+\beta\rho_2\left(\int_\Omega e_p^n\phi_x\,dx-\sum_{j=1}^{N}\left(((e_p^n)^+\phi^-)_{j+\frac12}+((e_p^n)^+\phi^+)_{j-\frac12}\right)\right)\\ &\quad-\sum_{i=1}^{n-1}(b_{n-i-1}-b_{n-i})\int_\Omega(3e_T^i-4e_T^{i-1}+e_T^{i-2})\phi\,dx\\ &\quad-2\Delta t\,b_{n-1}\int_\Omega e_v^0\phi\,dx-4\int_\Omega e_T^{n-1}\phi\,dx+\int_\Omega e_T^{n-2}\phi\,dx\\ &\quad-2\Delta t\sum_{i=1}^{n-1}(b_{n-i-1}-b_{n-i})\int_\Omega e_T^i\phi\,dx-2\Delta t\,b_{n-1}\int_\Omega e_T^0\phi\,dx\\ &\quad+\beta\int_\Omega\gamma^n\phi\,dx+\int_\Omega e_p^n w\,dx+\int_\Omega e_T^n w_x\,dx\\ &\quad-\sum_{j=1}^{N}\left(((e_T^n)^-w^-)_{j+\frac12}+((e_T^n)^-w^+)_{j-\frac12}\right)=0. \end{aligned} \tag{3.16}$$

Inserting the decomposition Eq (3.15) into the above identity leads to the reformulated error equation

$$
\begin{aligned}
&(\rho_1+3+2\Delta t)\int_\Omega \xi_T^n\phi\,dx+\beta\rho_2\left(\int_\Omega \xi_p^n\phi_x\,dx-\sum_{j=1}^{N}\left(((\xi_p^n)^+\phi^-)_{j+\frac12}+((\xi_p^n)^+\phi^+)_{j-\frac12}\right)\right)\\
&\quad+\int_\Omega \xi_p^n w\,dx+\int_\Omega \xi_T^n w_x\,dx-\sum_{j=1}^{N}\left(((\xi_T^n)^-w^-)_{j+\frac12}+((\xi_T^n)^-w^+)_{j-\frac12}\right)\\
&=\sum_{i=1}^{n-1}(b_{n-i-1}-b_{n-i})\int_\Omega(3\xi_T^i-4\xi_T^{i-1}+\xi_T^{i-2})\phi\,dx-2\Delta t\,b_{n-1}\int_\Omega e_v^0\phi\,dx\\
&\quad+4\int_\Omega \xi_T^{n-1}\phi\,dx-\int_\Omega \xi_T^{n-2}\phi\,dx-\beta\int_\Omega \gamma^n\phi\,dx+2\Delta t\,b_{n-1}\int_\Omega \xi_T^0\phi\,dx\\
&\quad+2\Delta t\sum_{i=1}^{n-1}(b_{n-i-1}-b_{n-i})\int_\Omega \xi_T^i\phi\,dx-\sum_{i=1}^{n-1}(b_{n-i-1}-b_{n-i})\int_\Omega(3\eta_T^i-4\eta_T^{i-1}+\eta_T^{i-2})\phi\,dx\\
&\quad-4\int_\Omega \eta_T^{n-1}\phi\,dx+\int_\Omega \eta_T^{n-2}\phi\,dx+(\rho_1+3+2\Delta t)\int_\Omega \eta_T^n\phi\,dx\\
&\quad-2\Delta t\sum_{i=1}^{n-1}(b_{n-i-1}-b_{n-i})\int_\Omega \eta_T^i\phi\,dx-2\Delta t\,b_{n-1}\int_\Omega \eta_T^0\phi\,dx\\
&\quad+\beta\rho_2\left(\int_\Omega \eta_p^n\phi_x\,dx-\sum_{j=1}^{N}\left(((\eta_p^n)^+\phi^-)_{j+\frac12}+((\eta_p^n)^+\phi^+)_{j-\frac12}\right)\right)\\
&\quad+\int_\Omega \eta_p^n w\,dx+\int_\Omega \eta_T^n w_x\,dx-\sum_{j=1}^{N}\left(((\eta_T^n)^-w^-)_{j+\frac12}+((\eta_T^n)^-w^+)_{j-\frac12}\right).
\end{aligned}
$$

Now we select the test functions as $\phi=\xi_T^n$ and $w=\beta\rho_2\xi_p^n$ in the error equation above. By using the projection properties stated in Eq (2.1), we obtain the following estimate:

$$
\begin{aligned}
&(\rho_1+3+2\Delta t)\|\xi_T^n\|^2+\beta\rho_2\|\xi_p^n\|^2\\
&\quad\le\sum_{i=1}^{n-1}(b_{n-i-1}-b_{n-i})(3\|\xi_T^i\|+4\|\xi_T^{i-1}\|+\|\xi_T^{i-2}\|)\|\xi_T^n\|\\
&\quad\quad+2\Delta t\,b_{n-1}\|e_v^0\|\|\xi_T^n\|+4\|\xi_T^{n-1}\|\|\xi_T^n\|+\|\xi_T^{n-2}\|\|\xi_T^n\|+\beta\|\gamma^n\|\|\xi_T^n\|\\
&\quad\quad+2\Delta t\sum_{i=1}^{n-1}(b_{n-i-1}-b_{n-i})\|\xi_T^i\|\|\xi_T^n\|+2\Delta t\,b_{n-1}\|\xi_T^0\|\|\xi_T^n\|\\
&\quad\quad+\sum_{i=1}^{n-1}(b_{n-i-1}-b_{n-i})(3\|\eta_T^i\|+4\|\eta_T^{i-1}\|+\|\eta_T^{i-2}\|)\|\xi_T^n\|\\
&\quad\quad+4\|\eta_T^{n-1}\|\|\xi_T^n\|+\|\eta_T^{n-2}\|\|\xi_T^n\|+2\Delta t\,b_{n-1}\|\eta_T^0\|\|\xi_T^n\|\\
&\quad\quad+2\Delta t\sum_{i=1}^{n-1}(b_{n-i-1}-b_{n-i})\|\eta_T^i\|\|\xi_T^n\|\\
&\quad\quad+(\rho_1+3+2\Delta t)\|\eta_T^n\|\|\xi_T^n\|+\beta\rho_2\|\eta_p^n\|\|\mathcal{P}^-e_p^n\|.
\end{aligned}
\tag{3.17}
$$

Applying the elementary inequality $ab \le \frac{1}{4\varepsilon}a^2 + \varepsilon b^2$ together with $a^2 + b^2 \le (a+b)^2$, we directly deduce the following simplified bound:

$$\begin{aligned}
\|\xi_T^n\| \le & \sum_{i=1}^{n-1}(b_{n-i-1} - b_{n-i})(3\|\xi_T^i\| + 4\|\xi_T^{i-1}\| + \|\xi_T^{i-2}\|) + 2\Delta t\, b_{n-1}\|e_v^0\| \\
& + 4\|\xi_T^{n-1}\| + \|\xi_T^{n-2}\| + \|\gamma^n\| + 2\Delta t \sum_{i=1}^{n-1}(b_{n-i-1} - b_{n-i})\|\xi_T^i\| \\
& + 2\Delta t\, b_{n-1}\|\xi_T^0\| + \sum_{i=1}^{n-1}(b_{n-i-1} - b_{n-i})(3\|\eta_T^i\| + 4\|\eta_T^{i-1}\| + \|\eta_T^{i-2}\|) \\
& + 4\|\eta_T^{n-1}\| + \|\eta_T^{n-2}\| + 2\Delta t \sum_{i=1}^{n-1}(b_{n-i-1} - b_{n-i})\|\eta_T^i\| \\
& + 2\Delta t\, b_{n-1}\|\eta_T^0\| + (\rho_1 + 3 + 2\Delta t)\|\eta_T^n\| + \sqrt{\beta\rho_2}\,\|\eta_p^n\|.
\end{aligned} \tag{3.18}$$

We now establish the convergence of the scheme (3.7) using mathematical induction.

First, consider the base case $n = 1$ in inequality (3.17). This yields

$$\begin{aligned}
\|\xi_T^1\| \le & 2\Delta t\|e_v^0\| + 4\|\xi_T^0\| + \|\eta_T^{-1}\| + \|\gamma^1\| \\
& + 2\Delta t\|\xi_T^0\| + 4\|\eta_T^0\| + \|\eta_T^{-1}\| \\
& + 2\Delta t\|\eta_T^0\| + (\rho_1 + 3 + 2\Delta t)\|\eta_T^1\| \\
& + \sqrt{\beta\rho_2}\,\|\eta_p^1\|.
\end{aligned}$$

Taking into account the following approximation properties

$$\|e_T^0\| \le Ch^{k+1}, \quad \|e_v^0\| \le Ch^{k+1}, \quad \|e_T^{-1}\| \le C(h^{k+1} + (\Delta t)^2), \quad \|\gamma^1\| \le C(\Delta t)^{3-\alpha},$$

we directly arrive at

$$\|\xi_T^1\| \le C(h^{k+1} + (\Delta t)^{3-\alpha}). \tag{3.19}$$

Now assume that for all indices $m = 1, 2, \ldots, J$, the following estimate holds:

$$\|\xi_T^m\| \le C(h^{k+1} + (\Delta t)^{3-\alpha}). \tag{3.20}$$

Next, set $n = J + 1$ in Eq (3.17). We then obtain

$$\begin{aligned}
\|\xi_T^{J+1}\| \le & \sum_{i=1}^{J}(b_{J-i} - b_{J+1-i})(3\|\xi_T^i\| + 4\|\xi_T^{i-1}\| + \|\xi_T^{i-2}\|) + 2\Delta t\, b_J\|e_v^0\| \\
& + 4\|\xi_T^J\| + \|\xi_T^{J-1}\| + \|\gamma^{J+1}\| \\
& + 2\Delta t \sum_{i=1}^{J}(b_{J-i} - b_{J+1-i})\|\xi_T^i\| + 2\Delta t\, b_J\|\xi_T^0\| \\
& + \sum_{i=1}^{J}(b_{J-i} - b_{J+1-i})(3\|\eta_T^i\| + 4\|\eta_T^{i-1}\| + \|\eta_T^{i-2}\|) \\
& + 4\|\eta_T^J\| + \|\eta_T^{J-1}\| + 2\Delta t \sum_{i=1}^{J}(b_{J-i} - b_{J+1-i})\|\eta_T^i\| + 2\Delta t\, b_J\|\eta_T^0\| \\
& + \sqrt{\beta\rho_2}\,\|\eta_p^{J+1}\| + (\rho_1 + 3 + 2\Delta t)\|\eta_T^{J+1}\|.
\end{aligned}$$

Applying the induction hypothesis (3.20) together with the projection estimates (2.1) leads to

$$\|\xi_T^{J+1}\| \leq C(h^{k+1} + (\Delta t)^{3-\alpha}).$$

Finally, using the triangle inequality in combination with the interpolation properties (2.1), we conclude that Theorem 3.2 holds for all n. This completes the proof. □

4. Numerical experiments

In this section, we present numerical experiments to verify the accuracy and convergence properties of the proposed fully discrete DG method. We consider the time-fractional telegraph equation (1.1) on the space-time domain

$$(x, t) \in [0, 1] \times [0, 1],$$

with the parameters

$$\rho_1 = 1, \qquad \rho_2 = 0.5, \qquad t_F = 1.$$

The exact solution is prescribed as

$$T(x, t) = t^2 \sin(2\pi x). \tag{4.1}$$

Accordingly, the initial conditions are

$$T(x, 0) = 0, \qquad T_t(x, 0) = 0,$$

and the exact solution satisfies the periodic boundary condition.

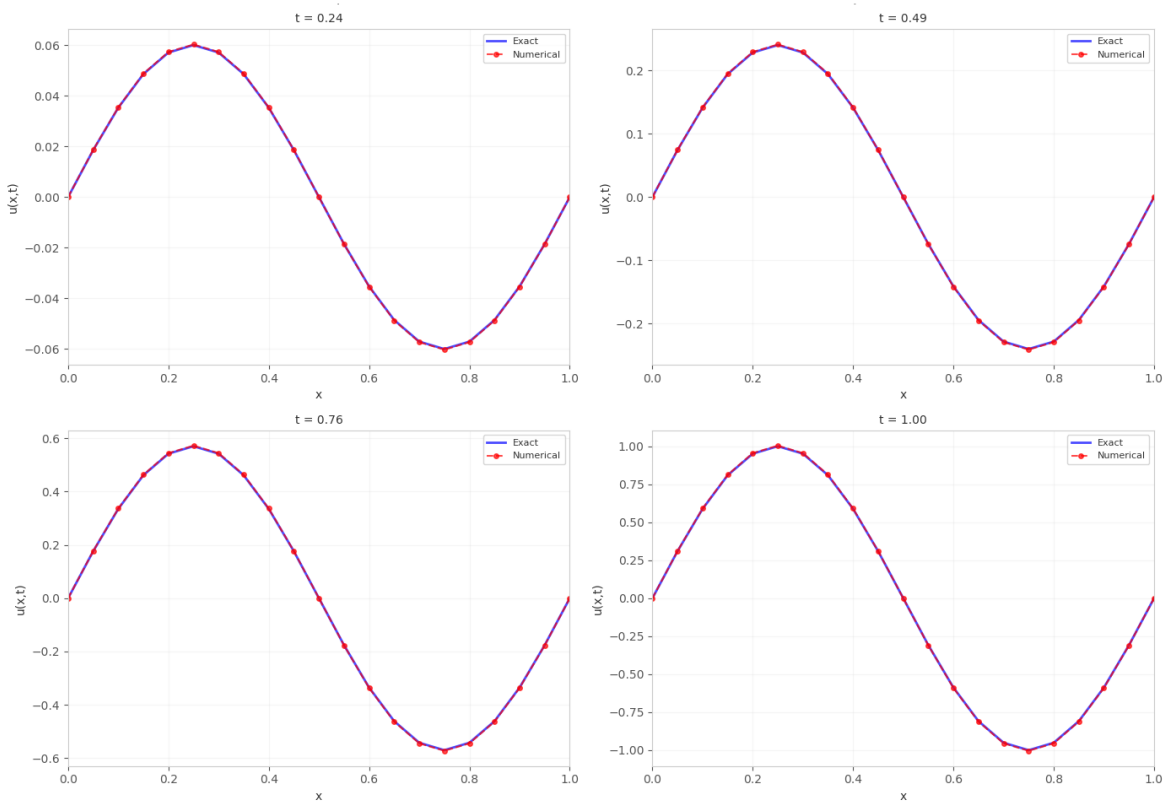


Figure 1. Comparison of numerical and exact solutions at different time steps.

The spatial domain $[0, 1]$ is partitioned into N uniform elements, and the temporal direction is discretized with $M = 1000$ steps to ensure that the spatial error dominates. The parameter of the generalized alternating numerical flux is chosen as $\theta = 0.3$ and $\theta = 0.7$.

The experimental convergence rate in space is computed by

$$\text{order} = \frac{\log(\|T - T_{h_1}\|/\|T - T_{h_2}\|)}{\log(h_1/h_2)},$$

where T is the exact solution, T_{h_i} is the numerical solution with spatial step size h_i, and $\|\cdot\|$ denotes either the L^2 or L^∞ norm.

Table 1. Spatial accuracy test using piecewise P^k polynomials with parameters $M = 1000, \theta = 0.3$.

α	P^k	N	L^2-error	Order	L^∞-error	Order
$\alpha = 1.2$	P^0	5	3.82349E-01	-	8.12655E-01	-
		10	2.03462E-01	0.91	4.38134E-01	0.89
		20	1.05191E-01	0.95	2.31452E-01	0.92
		40	5.39513E-02	0.96	1.18681E-01	0.96
	P^1	5	7.12147E-02	-	3.12599E-01	-
		10	1.82913E-02	1.96	8.24742E-02	1.92
		20	4.86453E-03	1.91	2.23942E-02	1.88
		40	1.28312E-03	1.92	5.90814E-03	1.92
	P^2	5	8.22316E-03	-	5.24166E-02	-
		10	1.11901E-03	2.87	7.72435E-03	2.76
		20	1.50242E-04	2.89	1.05153E-03	2.87
		40	1.99061E-05	2.91	1.37122E-04	2.93
$\alpha = 1.7$	P^0	5	3.15285E-001	-	7.92660E-001	-
		10	1.72828E-001	0.87	4.25657E-001	0.91
		20	9.24807E-002	0.91	2.27423E-001	0.92
		40	4.80164E-002	0.95	1.18048E-001	0.95
	P^1	5	6.92665E-002	-	2.98655E-001	-
		10	1.82241E-002	1.93	7.95277E-002	1.91
		20	4.81034E-003	1.92	2.13709E-002	1.89
		40	1.27107E-003	1.92	5.59445E-003	1.93
	P^2	5	7.89263E-003	-	5.01225E-002	-
		10	1.06313E-003	2.89	7.34222E-003	2.79
		20	1.43861E-004	2.91	1.01006E-003	2.88
		40	1.95918E-005	2.92	1.35686E-004	2.91

We apply the proposed method using piecewise P^k polynomials ($k = 0, 1, 2$) with the fractional order $\alpha = 1.2$ and $\alpha = 1.7$. The errors and convergence orders are listed in Tables 1 and 2 for $\theta = 0.3$ and $\theta = 0.7$, respectively. Additionally, Figure 1 presents the comparison between the numerical and exact solutions at different time instants, visually confirming the good agreement.

From the results, we observe that the spatial convergence rates for piecewise P^k polynomials ($k = 0, 1, 2$) agree well with the theoretical optimal orders. Specifically, the P^0 approximation yields an accuracy of approximately $O(h)$, the P^1 approximation achieves a clear second-order convergence $O(h^2)$, and the P^2 approximation achieves nearly third-order accuracy $O(h^3)$, with the computed orders for both $\alpha = 1.2$ and $\alpha = 1.7$ being close to the expected values of 1, 2, and 3, respectively. Moreover, no significant difference is observed between the results for $\theta = 0.3$ and $\theta = 0.7$, indicating that the spatial error dominates when the temporal mesh is sufficiently fine ($M = 1000$). These results demonstrate the high accuracy and robustness of the present method for solving the time-fractional telegraph equation.

Table 2. Spatial accuracy test using piecewise P^k polynomials with the parameters $M = 1000, \theta = 0.7$.

α	P^k	N	L^2-error	Order	L^∞-error	Order
$\alpha = 1.2$	P^0	5	3.72524E-001	-	7.98356E-001	-
		10	1.98263E-001	0.92	4.45890E-001	0.88
		20	1.03155E-001	0.95	2.36951E-001	0.91
		40	5.41810E-002	0.95	1.24230E-001	0.95
	P^1	5	7.26535E-002	-	3.22566E-001	-
		10	1.87286E-002	1.95	8.51145E-002	1.92
		20	4.92405E-003	1.92	2.25102E-002	1.91
		40	1.31967E-003	1.91	5.93601E-003	1.92
	P^2	5	8.15846E-003	-	5.21575E-002	-
		10	1.15931E-003	2.88	7.49749E-003	2.79
		20	1.55348E-004	2.89	1.00560E-003	2.89
		40	2.03741E-005	2.92	1.30552E-004	2.91
$\alpha = 1.7$	P^0	5	3.23256E-01	-	8.24638E-01	-
		10	1.75691E-01	0.88	4.35657E-01	0.92
		20	9.23600E-02	0.91	2.30100E-01	0.92
		40	4.74600E-02	0.96	1.20700E-01	0.93
	P^1	5	6.82555E-02	-	2.82558E-01	-
		10	1.80283E-02	1.92	7.46400E-02	1.92
		20	4.76100E-03	1.92	2.01400E-02	1.89
		40	1.26600E-03	1.91	5.25000E-03	1.94
	P^2	5	7.79258E-03	-	5.13594E-02	-
		10	1.06007E-03	2.88	7.42800E-03	2.79
		20	1.41000E-04	2.91	1.00200E-03	2.89
		40	1.85200E-05	2.93	1.32400E-04	2.92

5. Conclusions and future work

In this paper, we have developed and analyzed a fully discrete numerical method for solving the time-fractional telegraph equation of order α with $1 < \alpha < 2$. The proposed scheme combines a finite

difference discretization in time with a DG method in space, where generalized alternating numerical fluxes are used to enhance flexibility and accommodate nonsymmetric flux choices. The temporal discretization is based on a second-order backward difference formula for the first-order derivative, which, together with the fractional derivative approximations, leads to a fully implicit time-stepping scheme. The spatial discretization is handled by the DG method using piecewise polynomial spaces of degree k, yielding high-order accuracy in space.

The main theoretical contributions of this work are twofold. First, we have established the unconditional stability of the fully discrete scheme, showing that the numerical solution remains bounded independently of the time step size and mesh size. Second, we have derived optimal error estimates demonstrating that the method achieves a convergence rate of $O(h^{k+1} + (\Delta t)^{3-\alpha})$, where h denotes the maximum mesh size and Δt the time step. These theoretical results are supported by the properties of the generalized Gauss–Radau projection and the careful treatment of the initial conditions.

Numerical experiments have been presented to validate the theoretical findings, illustrating the robustness, reliability, and high-order accuracy of the proposed method. The results confirm that the method performs well for various parameter choices and effectively captures the memory effects inherent in fractional-order systems.

Despite the encouraging results obtained, several directions remain open for future investigation. First, although the present analysis is restricted to uniform spatial and temporal grids, the proposed method can, in principle, be extended to nonuniform meshes. For nonuniform spatial meshes, the DG formulation remains applicable, but the generalized Gauss–Radau projection estimates need to be reformulated in terms of local mesh sizes. For nonuniform temporal meshes, the convolution weights of the Caputo derivatives depend on the individual time steps, and the positivity and monotonicity properties used in the present stability and convergence analyses need to be re-established. In particular, graded or adaptive temporal meshes may be useful for problems with weak initial singularities. Second, the extension of the proposed method to two- or three-dimensional problems on complex geometries is of practical interest, although the increased dimensionality poses additional challenges in terms of computational cost and implementation complexity. Third, the development of efficient fast algorithms for evaluating the history terms of the fractional derivatives would be valuable for large-scale simulations. Finally, the generalization of the present method to other classes of fractional differential equations, including multiterm and variable-order fractional equations, represents another promising direction for future research.

Use of AI tools declaration

The authors declare they have not used artificial intelligence (AI) tools in the creation of this article.

Conflicts of interest

The authors declare there is no conflict of interest.

Acknowledgement

This work was supported by the Henan Province Science and Technology Research Project(262102220043).

Author contributions

Miaomiao Yang: Investigation, methodology, writing–original draft, review and editing, programming, supervision. Xiao Chen: writing–original draft, investigation, formal analysis, revision and editing. All authors read and approved the final manuscript.

References

1. C. P. Li, F. H. Zeng, *Numerical Methods for Fractional Calculus*, CRC Press, Boca Raton, FL, 2015.
2. L. Wei, L. Feng, I. Turner, Z. Mao, F. Liu, Numerical investigation of the 2D unsteady natural convection heat transfer equation with tempered fractional constitutive relationship, *Commun. Nonlinear Sci. Numer. Simul.*, **161** (2026), 110071. https://doi.org/10.1016/j.cnsns.2026.110071
3. E. Sousa, C. Li, A weighted finite difference method for the fractional diffusion equation based on the Riemann–Liouville derivative, *Appl. Numer. Math.*, **90** (2015), 22–37. https://doi.org/10.1016/j.apnum.2014.11.007
4. M. Stynes, E. O'Riordan, J. Gracia, Error analysis of a finite difference method on graded meshes for a time-fractional diffusion equation, *SIAM J. Numer. Anal.*, **55** (2017), 1057–1079. https://doi.org/10.1137/16M1082329
5. L. Qiao, J. Guo, W. Qiu, Fast BDF2 ADI methods for the multi-dimensional tempered fractional integrodifferential equation of parabolic type, *Comput. Math. Appl.*, **123** (2022), 89–104. https://doi.org/10.1016/j.camwa.2022.08.014
6. X. D. Zhang, Y. L. Feng, Z. Y. Luo, J. Liu, A spatial sixth-order numerical scheme for solving fractional partial differential equation, *Appl. Math. Lett.*, **159** (2025), 109265. https://doi.org/10.1016/j.aml.2024.109265
7. Z. Wang, X. Deng, Y. Mo, Nonuniform $L2\text{-}1_\sigma$ method combined with time two-grid algorithm for the time fractional Gray–Scott model with initial singularity, *J. Comput. Appl. Math.*, **480** (2026), 117258. https://doi.org/10.1016/j.cam.2025.117258
8. S. Maji, S. Natesan, Nonsymmetric interior penalty Galerkin method for nonlinear time-fractional integro-partial differential equations, *Math. Comput. Simul.*, **213** (2023), 1–17. https://doi.org/10.1016/j.matcom.2023.05.020
9. W. H. Deng, J. S. Hesthaven, Local discontinuous Galerkin methods for fractional diffusion equations, *ESAIM Math. Model. Numer. Anal.*, **47** (2013), 1845–1864. https://doi.org/10.1051/m2an/2013091
10. L. Wei, L. Liu, X. Zhang, An upwind interior penalty DG scheme for solute transport in 2D variable-order mobile–immobile model, *Entropy*, **28** (2026), 997. https://doi.org/10.3390/e28090997

11. Y. Du, Y. Liu, H. Li, Z. Fang, S. He, Local discontinuous Galerkin method for a nonlinear time-fractional fourth-order partial differential equation, *J. Comput. Phys.*, **344** (2017), 108–126. https://doi.org/10.1016/j.jcp.2017.04.078
12. H. Wang, D. Yang, S. Zhu, Inhomogeneous Dirichlet boundary-value problems of space-fractional diffusion equations and their finite element approximations, *SIAM J. Numer. Anal.*, **52** (2014), 1292–1310. https://doi.org/10.1137/130932776
13. S. Chen, J. Shen, L. L. Wang, Generalized Jacobi functions and their applications to fractional differential equations, *Math. Comput.*, **85** (2016), 1603–1638.
14. X. Li, C. Xu, A space-time spectral method for the time fractional diffusion equation, *SIAM J. Numer. Anal.*, **47** (2009), 2108–2131. https://doi.org/10.1137/080718942
15. Y. M. Lin, C. J. Xu, Finite difference/spectral approximations for the time-fractional diffusion equation, *J. Comput. Phys.*, **225** (2007), 1533–1552. https://doi.org/10.1016/j.jcp.2007.02.001
16. R. Huang, Z. Weng, J. Yuan, Numerical approximation of nonlinear time fractional parabolic optimal control problems based on a collocation technique, *Numer. Algorithms*, 2026. https://doi.org/10.1007/s11075-026-02418-4
17. R. Huang, Z. Weng, J. Yuan, Collocation-based numerical simulation of multi-dimensional nonlinear time-fractional Schrödinger equations, *Comput. Math. Appl.*, **183** (2025), 214–233. https://doi.org/10.1016/j.camwa.2025.02.002
18. S. Kumar, A new analytical modelling for telegraph equation via Laplace transform, *Appl. Math. Modell.*, **38** (2014), 3154–3163. https://doi.org/10.1016/j.apm.2013.11.035
19. L. Beghin, E. Orsingher, The telegraph process stopped at stable-distributed times connection with the fractional telegraph equation, *Fract. Calc. Appl. Anal.*, **6** (2003), 187–204.
20. E. Orsingher, L. Beghin, Time-fractional telegraph equation and telegraph processes with Brownian time, *Probab. Theory Relat. Fields*, **128** (2004), 141–160. https://doi.org/10.1007/s00440-003-0309-8
21. J. Chen, F. Liu, V. Anh, Analytical solution for the time-fractional telegraph equation by the method of separating variables, *J. Math. Anal. Appl.*, **338** (2008), 1364–1377. https://doi.org/10.1016/j.jmaa.2007.06.023
22. S. Momani, Analytic and approximate solutions of the space- and time-fractional telegraph equations, *Appl. Math. Comput.*, **170** (2005), 1126–1134. https://doi.org/10.1016/j.amc.2005.01.009
23. W. Jiang, Y. Lin, Representation of exact solution for the time-fractional telegraph, *Commun. Nonlinear Sci. Numer. Simul.* , **16** (2011), 3639–3645. https://doi.org/10.1016/j.cnsns.2010.12.019
24. J. Biazar, H. Ebrahimi, Z. Ayati, An approximation to the solution of telegraph equation by variational iteration method, *Numer. Methods Partial Differ. Equ.*, **25** (2009), 797–801. https://doi.org/10.1002/num.20373
25. A. Yildirim, He's homotopy perturbation method for solving the space and time fractional telegraph equations, *Int. J. Comput. Math.*, **87** (2010), 2998–3006. https://doi.org/10.1080/00207160902874653

26. Y. Zhang, Z. Wang, Numerical simulation for time-fractional diffusion-wave equations with time delay, *J. Appl. Math. Comput.*, **69** (2023), 137–157. https://doi.org/10.1007/s12190-022-01739-6

27. C. Ou, Z. Wang, S. Vong, A second-order fitted scheme combined with time two-grid technique for two-dimensional nonlinear time fractional telegraph equations involving initial singularity, *J. Comput. Appl. Math.*, **448** (2024), 115936. https://doi.org/10.1016/j.cam.2024.115936

28. L. Wei, Y. Chen, F. Qin, J. Huang, P. Li, The discontinuous Galerkin method for solving the two-dimensional transport equation with distributed-order memory kernel on triangular meshes, *Appl. Numer. Math.*, **228** (2026), 57–70. https://doi.org/10.1016/j.apnum.2026.05.009

29. I. Podlubny, *Fractional Differential Equations*, Academic Press, New York, 1999.

30. Y. Cheng, X. Meng, Q. Zhang, Application of generalized Gauss-Radau projections for the local discontinuous Galerkin method for linear convection-diffusion equations, *Math. Comput.*, **86** (2017), 1233–1267. https://doi.org/10.1090/mcom/3141

31. L. Wei, Y. He, A fully discrete local discontinuous Galerkin method with the generalized numerical flux to solve the tempered fractional reaction-diffusion equation, *Discrete Contin. Dyn. Syst. Ser. B*, **26** (2021), 4907–4926. https://doi.org/10.3934/dcdsb.2020319

32. L. Wei, Y. Yang. Optimal order finite difference/local discontinuous Galerkin method for variable-order time-fractional diffusion equation, *J. Comput. Appl. Math.*, **383** (2021), 113129. https://doi.org/10.1016/j.cam.2020.113129



AIMS Press

© 2026 the Author(s), licensee AIMS Press. This is an open access article distributed under the terms of the Creative Commons Attribution License (https://creativecommons.org/licenses/by/4.0)